Molecular Dynamics Simulations of Bimolecular Electron Transfer: Testing the Coulomb Term in the Weller Equation

Rumble, Christopher Allen; Licari, Giuseppe Léonardo; Vauthey, Eric

How to cite

RUMBLE, Christopher Allen, LICARI, Giuseppe Léonardo, VAUTHEY, Eric. Molecular Dynamics Simulations of Bimolecular Electron Transfer: Testing the Coulomb Term in the Weller Equation. In: Journal of Physical Chemistry. B, Condensed Matter, Materials, Surfaces, Interfaces and Biophysical, 2020, vol. 124, n° 44, p. 9945–9950. doi: 10.1021/acs.jpcb.0c09031

This publication URL: https://archive-ouverte.unige.ch//unige:144341
Publication DOI: 10.1021/acs.jpcb.0c09031

Molecular Dynamics Simulations of Bimolecular Electron Transfer: Testing the Coulomb Term in the Weller Equation

Christopher A. Rumble,[*,†] Giuseppe Licari,[†,‡] and Eric Vauthey[*,†]

†*Department of Physical Chemistry, University of Geneva, 30 Quai Ernest-Ansermet, CH-1211 Geneva, Switzerland*

‡*Current address: NIH Center for Macromolecular Modeling and Bioinformatics, Beckman Institute for Advanced Science and Technology, Department of Biochemistry, Center for Biophysics and Quantitative Biology, University of Illinois at Urbana-Champaign, Urbana, Illinois, USA*

E-mail: christopher.rumble@unige.ch; eric.vauthey@unige.ch

Abstract

Reliable estimation of the driving force of photoinduced electron transfer between neutral reactants is of utmost importance for most practical applications of these reactions. The driving force is usually calculated from the Weller equation which contains a Coulomb term, C, whose magnitude in polar solvents is debated. We have performed umbrella sampling molecular dynamics simulations in order to determine C from the potentials of mean force between neutral and ionic donor/acceptor pairs of different sizes in solvents of varying polarity. According to the simulations, C in polar solvents is a factor of 2 more negative than typically calculated according to the Weller equation. Use of the π-stack contact distance in the Weller equation instead of the van der Waals radius recovers the correct value of C, but this is mostly fortuitous due to the compensating effects of overestimating the dielectric screening at contact and neglecting both charge dilution and desolvation.

1 Introduction

The long-standing interest in photoinduced electron transfer (ET) is driven not only by the desire to understand the details of this fundamental reaction but also by the potential benefits resulting from its applications in many technological areas.[1–13] Knowledge of the ET driving force, -ΔG_{ET}, is of utmost importance for estimating the feasibility of this process, for predicting its rate constant using *e.g.* Marcus theory, and for evaluating what fraction of the absorbed light is eventually converted into chemical energy. To illustrate the importance of good estimations of ΔG_{ET}, the semiclassical Marcus expression[14] predicts that variations of ΔG_{ET} within $\pm$0.1 eV can change the ET rate constant, k_{ET} by almost 2 orders of magnitude, depending on the relative magnitudes of the reorganization energy and driving force.

The determination of ΔG_{ET} is generally based on the Weller equation, which, for ET

between two neutral reactants, is given by:[15,16]

$$\Delta G_{\mathrm{ET}} = -E^{*} + e\left[E_{\mathrm{ox}}(D) - E_{\mathrm{red}}(A)\right] + C, \tag{1}$$

where E^{*} is the energy of the excited reactant, $E_{\mathrm{ox}}(D)$ and $E_{\mathrm{red}}(A)$ are the redox potentials of the electron donor (D) and acceptor (A), respectively, and C accounts for the free energy gained upon bringing the charged products at ET distance minus the free energy for the same process but for the neutral reactants. The first two terms of Eq. 1 rely on the assumption that the redox potential of a photoexcited D/A pair can be approximated by the sum of the excited-state energy and the ground-state redox potentials, which was shown to be a reasonable assumption by Fox and coworkers.[17] Given the aforementioned sensitivity of k_{ET} to ΔG_{ET}, knowledge of the magnitude of C and its dependence on solvent polarity and reactant size is crucial for quantitatively describing ET dynamics.

The C term of Eq. 1 is typically calculated using Coulomb's law:

$$C = -\frac{e^{2}}{4\pi\varepsilon_{0}\varepsilon_{\mathrm{s}}r}, \tag{2}$$

where e the elementary charge, ε_{0} the vacuum permittivity, ε_{s} the dielectric constant of the solvent, and r the interionic distance. Eq. 2 is based on the dielectric continuum model and assumes the ions can be described as point charges with opposite unit charge. In highly polar solvents such as acetonitrile, C is predicted to be small, relative to the other three terms of Eq. 1, even for two ions at contact. For example, for $r = 0.70$ nm, a separation typically assumed for aromatic donor/acceptor pairs, Eq. 2 predicts a stabilization energy of about -0.05 eV in ACN. For this reason, this Coulomb term is often neglected in polar media.[18,19]

However, Suppan suggested that Eq. 2 strongly underestimates the electrostatic stabilization at contact distance in polar solvents, especially with aromatic reactants.[20] He proposed that screening of the charges arises mostly from the polarizability of the ions and that ε_{s} in

Eq. 2 should be replaced by n^2, where n is the refractive index of the ions. This conclusion was challenged by Tachiya,[21] who remarked that the term C in Weller equation should also account for the loss of solvation energy upon bringing two ions close together. Based on the dielectric continuum model with spherical reactants, he concluded that this loss of solvation energy is larger than the gain of electrostatic stabilization and that, consequently, C would be expected to be positive, with $C = 0.14\,\mathrm{eV}$ in acetonitrile at $r = 0.60\,\mathrm{nm}$.

Experimental verifications of the Weller equation are scarce. In principle, ΔG_{ET} could be determined from the equilibrium constant between reactants and products, whereas in practice, this is only possible for ΔG_{ET} around zero.[22,23] It is also generally accepted that ET in this case is not complete, and the product should be considered as an exciplex rather than a pair of ions.[24–29] More direct determination of ΔG_{ET} using time-resolved calorimetry was shown to be hampered by the estimation of the entropy change upon ET.[30–32]

These controversies on the nature and magnitude of C, along with the difficulty of accessing it experimentally, spurred the use of molecular dynamics (MD) simulations. The term C in Eq. 1 can be accessed from the potentials of mean force (PMF) between the charged products, $w_{\mathrm{C}}(r)$, and that of the neutral reactants, $w_{\mathrm{N}}(r)$. These functions reflect the free energy gained or lost when bringing the reactants or products to a given distance r in the solvent of interest.[33,34] In an MD simulation, the value of C at center-of-mass separation r can be estimated from the difference between $w_{\mathrm{C}}(r)$ and $w_{\mathrm{N}}(r)$:

$$C_{\mathrm{MD}}(r) = \Delta w(r) = w_{\mathrm{C}}(r) - w_{\mathrm{N}}(r). \tag{3}$$

In his theoretical investigation of the photoinduced ET, Ando used MD simulations to determine $w_{\mathrm{N}}(r)$ and $w_{\mathrm{C}}(r)$ for the D/A pair of *N*,*N*-dimethylaniline (DMA) and anthracene (ANT) in acetonitrile.[35] According to his simulations, C amounts to about -0.5 eV at contact distance and does not change significantly upon increasing the separation up to 1.2 nm. This surprising outcome was contradicted by later MD simulations of the same system by Hilczer

and Tachiya,[36] who introduced a constraint to maintain a face-to-face mutual orientation of ANT and DMA. Contrary to Ando, their PMF for the charged products points to a stabilization of the ions by -0.21 eV at contact distance (0.41 nm) decreasing to zero around 0.9–1.0 nm. These simulations were performed in acetonitrile and cyclohexane with a single D/A pair. Although these authors were able to test the influence of solvent polarity on C, the effects of the reactant size and conformational freedom were not investigated.

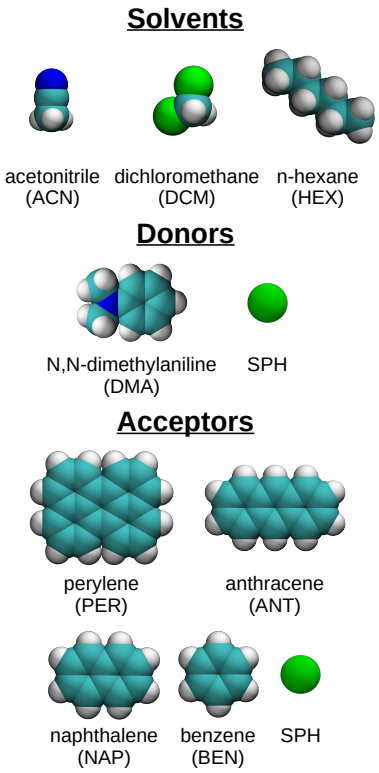

Chart 1: Space filling models of the simulated electron donor, acceptors and solvents.

Given the apparently contradictory results of previous studies and the advances in computational power in the last two decades as well as the need for a reliable estimation of this quantity, we have conducted a systematic investigation of the effect of solvent and reactant size and shape on the C term in Weller equation. We have conducted umbrella sampling MD simulations of a number of D/A/solvent systems, illustrated in Chart 1, in order to determine C from simulations of $w_{\mathrm{N}}(r)$ and $w_{\mathrm{C}}(r)$. Acetonitrile (ACN), dichloromethane (DCM), and n-hexane (HEX) were selected as solvents in order to study highly, medium, and non-polar

solvents. The donor was *N*,*N*-dimethylaniline (DMA) as in the previous studies,[35,36] and benzene (BEN), napthalene (NAP), anthracene (ANT), and perylene (PER) were selected as acceptors. These acceptors allow the reactant size to be systematically varied among solute sizes commonly encountered in experimental studies of ET. A pair of small spherical reactants (SPH) were also investigated for comparison with the molecular pairs.

2 Methods

Full details of the simulations are described in the Supporting Information (SI), and a brief description is provided here. The OPLS-AA force-field[37,38] was used for the solvents as well as for the solute non-bonded parameters. Although the use of a non-polarizable force-field may be questionable due to its weakness in properly describing π-stacks, we have previously demonstrated[39] that a similar simulation approach employing the same force-field can be used to reproduce the experimental absorption spectrum and ultrafast excited state conformational dynamics of an electron donor/acceptor pair. The success of this model in reproducing these experimental observables gives us confidence that the non-polaizable OPLS-AA force-field provides a reasonably good description of the energetics and structures of neutral and ionic pairs of the size studied here. Solute point charges were determined using CHELPG fits of electrostatic potentials generated by DFT calculations. For the spherical reactants, SPH, the OPLS-AA parameters for chloride were chosen and the charge modified accordingly. The umbrella sampling simulations were performed with GROMACS 2018.1 and the WHAM procedure was used to construct the PMFs. All simulations were carried out at 298 K, for which $k_{\mathrm{B}}T = 0.0257\,\mathrm{eV}$.

3 Results and Discussion

3.1 Potentials of mean forces (PMFs)

Figure 1 shows PMFs obtained for the neutral reactant pairs in ACN as well as the charged pairs in ACN and HEX. Figures S1-S2 contain PMFs for all other simulated D/A/solvent systems. For the spherical reactants, $w_{\mathrm{N}}(r)$ exhibits a minimum of approximately $k_{\mathrm{B}}T$ at a contact distance of $r = 0.45\,\mathrm{nm}$. The PMFs of the molecular reactants reflect a weak attraction in all solvents, with a minimum that does not significantly exceed $k_{\mathrm{B}}T$. In most cases, the minimum is at a distance that corresponds to a T-shaped mutual orientation of the reactants. However, for PER/DMA in ACN and HEX, this minimum is at a shorter distance that corresponds to a π-stacked geometry. In any case, these structures are not stable at room temperature, and a broad distribution of mutual orientations and distances can be anticipated.

The PMFs of the charged products (middle and bottom panels, Figure 1), are characterized by significantly deeper absolute minima even in highly polar ACN. The simulations of $\mathrm{SPH}^+/\mathrm{SPH}^-$ in ACN predict a second, shallower, minimum near 0.80 nm separated from the absolute minimum by a $1.7\,k_{\mathrm{B}}T$ barrier. This is indicative of a relatively stable conformation with a layer of solvent molecules between the two ions, which can be viewed as a solvent-separated ion-pair (SSIP). The relative stability of the SSIP in ACN can be explained by a balance between the solvation and Coulomb energies. Due to the molecularity of the solvent, a small decrease from the SSIP distance disrupts the solvent structure. This leads to a loss of solvation energy that is not compensated for by the gain in Coulomb energy, thus, a barrier between the SSIP and the contact ion-pair (CIP) appears. Contrary to the spherical ions, none of the molecular ions exhibit a local minimum at a distance corresponding to an SSIP. This indicates that molecular SSIPs should not be considered as distinct intermediates in bimolecular ET reactions with well-defined structures and lifetimes, as is sometimes assumed when discussing ion-pairs dynamics upon photoinduced ET.[40–42] As shown in several

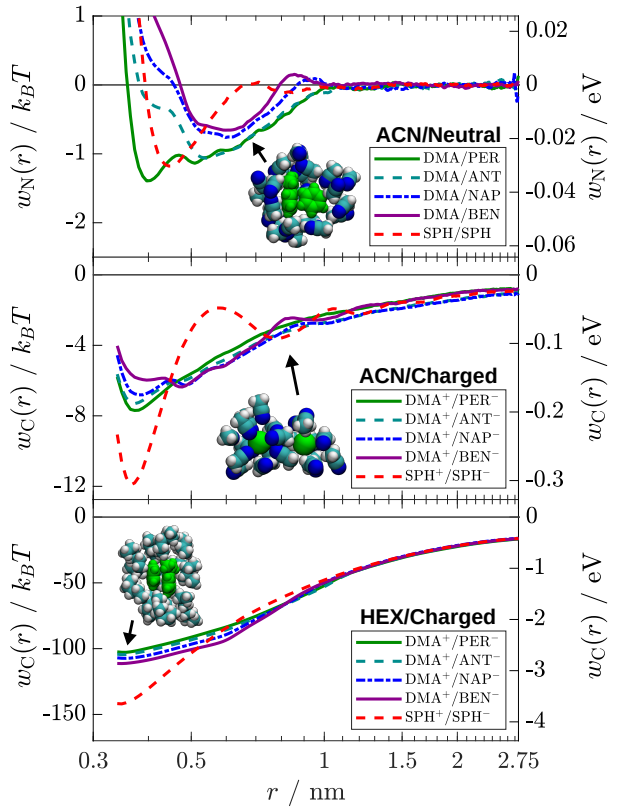

Figure 1: Potentials of mean force for five neutral reactant pairs, $w_{\mathrm{N}}(r)$, in ACN (top) and five charged product pairs, $w_{\mathrm{C}}(r)$, in ACN (middle) and HEX (bottom). The inset images are snapshots of DMA/BEN at $r = 0.55\,\mathrm{nm}$ (top), $\mathrm{SPH}^{+}/\mathrm{SPH}^{-}$ at $r = 0.85\,\mathrm{nm}$ (middle), and $\mathrm{DMA}^{\cdot+}/\mathrm{BEN}^{\cdot-}$ at $r = 0.35$ nm (bottom) with all solvent molecules within 0.5 nm. Solvent molecules situated between the viewer and the solutes have been removed for clarity.

studies,[43–45] ion-pair dynamics are better described using diffusion-reaction models.

The shape of $w_{\mathrm{C}}(r)$ for the molecular ion-pairs in ACN exhibits a significant dependence on the acceptor size. For BEN, the smallest molecular acceptor studied here, $w_{\mathrm{C}}(r)$ is characterized by a broad basin between 0.37 and 0.50 nm. The absolute minimum at 0.48 nm corresponds to a T-shaped mutual orientation of the ions with $\mathrm{DMA}^{\cdot+}$ molecular plane orthogonal to that of $\mathrm{BEN}^{\cdot-}$. However, the π-stacked geometry is only $0.5\,k_{\mathrm{B}}T$ higher in energy. For NAP, the deepest PMF minimum is at the π-stacked geometry, which is just $0.5\,k_{\mathrm{B}}T$ below that of the T-shaped structure. Finally, $w_{\mathrm{C}}(r)$ of ANT and PER, the largest acceptors, shows a single minimum at the π-stacked geometry. The depth of the minimum increases with increasing acceptor size, reflecting the enhanced stabilization of the π-stack geometry through dispersion interactions upon increasing the surface area of the acceptor.

For the same reason, the minimum moves from T-shaped to π-stacked geometries upon increasing acceptor size.

The ion-pair PMFs in non-polar HEX (bottom panel, Figure 1) are characterized by a deep minimum at 0.37 nm, indicative of a π-stacked geometry. For the spherical ions, the minimum increases from 12 to 142 $k_{\mathrm{B}}T$ when going from ACN to HEX. The depth of $w_{\mathrm{C}}(r)$ is significantly shallower for the molecular pairs than for the spherical pair and decreases from 111 to 103 $k_{\mathrm{B}}T$ with increasing acceptor size. This can be explained by the dilution of the charge upon increasing the anion size and the consequently smaller Coulomb attraction. Upon increasing the solvent polarity to DCM (Figure S3), the minimum of the PMFs remains at a distance corresponding to a π-stacked geometry, but with significantly shallower minima of $\sim$26 $k_{\mathrm{B}}T$. In both DCM and HEX the solvation energy is smaller and the Coulomb attraction larger than in ACN. Consequently, DCM and HEX can not effectively stabilize SSIPs and all ion-pairs simply collapse to CIPs.

3.2 Estimation of C

Next, we will use $\Delta w(r)$ to predict C from the simulations and compare them with C as calculated from Eq. 2. We define C_{MD} as the value of $\Delta w(r)$ at the simulated ion-pair contact distance r_{MD}, taken here to be the r corresponding to the minimum of $w_{\mathrm{C}}(r)$. For the Eq. 2 predictions, experimentalists typically estimate C using the van der Waals radius of the ion-pair, r_{vdW}, which we will call $C(r_{\mathrm{vdW}})$. Due to the profoundly non-spherical shape of the ions, especially for pairs such as DMA/PER and DMA/ANT, we also calculate C from Eq. 2 using r_{MD}, termed $C(r_{\mathrm{MD}})$. Values of r_{MD} and r_{vdW} are provided in Tables S1 and S2, respectively. When using Eq. 2, we employ an effective dielectric constant determined from fits of $w_{\mathrm{C}}(r)$ to Eq. 2 at large r in the solvent of interest (Section S3). Values of the three predictions for each D/A/solvent system are plotted in Figure 2 and tabulated in Table S3. Additionally, plots of all $\Delta w(r)$ and Eq. 2 predictions are provided in Figure S4.

These data reveal that, for the molecular pairs, C_{MD} is systematically 1.5–2 times more

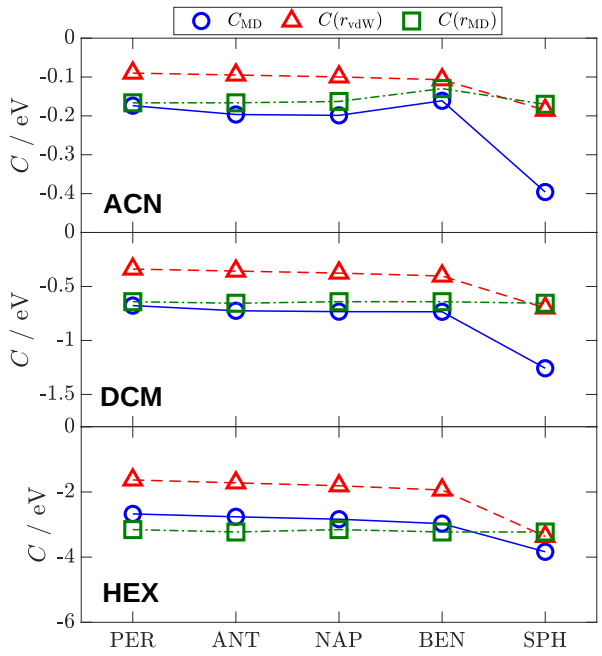

Figure 2: Coulomb terms obtained from the MD simulations, C_{MD}, and calculated from Eq. 2 with the sum of the van der Waals radii, $C(r_{\mathrm{vdW}})$, or the contact distance obtained from the MD simulations, $C(r_{\mathrm{MD}})$, in ACN (top), DCM (middle) and HEX (bottom).

negative than $C(r_{\mathrm{vdW}})$ in all solvents. This makes C_{MD} on average 0.11 eV more negative than $C(r_{\mathrm{vdW}})$ in ACN, 0.39 eV in DCM, and 0.92 eV in HEX. As discussed earlier, the simulated $w_{\mathrm{C}}(r)$ predict that the most stable mutual orientation of the molecular ions is a π-stacked geometry with a separation significantly smaller than r_{vdW} (Tables **??** and **??**). When r_{MD} is used instead of r_{vdW}, C_{MD} and $C(r_{\mathrm{MD}})$ are in agreement for the molecular ions to within $\sim 20\%$. For the spheres, r_{MD} and r_{vdW} are nearly identical, and therefore so are $C(r_{\mathrm{vdW}})$ and $C(r_{\mathrm{MD}})$. In this case, substitution of r_{MD} for r_{vdW} does not recover C_{MD} which is a factor of 2 more negative in ACN and DCM, and a factor of 1.2 in HEX than both Eq. 2 predictions. In order to quantify the practical implications of selecting the correct value of C, we used the classical non-adiabatic Marcus expression to make predictions of k_{ET} using the three versions of C described above for the DMA/PER system.[14] As detailed in Section S5 and Figure S7, these variations in C can change the predicted values of k_{ET} by several orders of magnitude. Therefore, if quantitative descriptions of ET processes are required, these seemingly small variations in C must be considered, as they can have profound effects on

the magnitude of k_{ET}.

3.3 Shortcomings of using Coulomb's Law for describing C

The data presented in Figure 2 lead us to ask: why does Eq. 2 appear to make reasonable predictions of C for molecular ions (when the correct ionic radius is used), but the predictions for the spheres are poor regardless in all cases? As discussed earlier, Eq. 2 is based on a model of point charges immersed in a dielectric continuum with no volume associated with either the solute or solvent. In such a model, ions at contact would still have the dielectric medium, *i.e.* solvent molecules, embedded between them. When ions with volume are brought into contact in a molecular solvent all solvent molecules are forced out of the interstitial region. The excluded solvent can no longer easily screen the ion charges, and the magnitude of ε_S is effectively decreased. This results in a Coulomb force that is stronger than predicted by Eq. 2, and C_{MD} becomes significantly more negative than $C(r_{\mathrm{vdW}})$ and $C(r_{\mathrm{MD}})$. Concomitantly, the molecular ion pairs do not deviate as strongly from from Eq. 2. Unlike the atomic ions, the two excess charges of the molecular ions are distributed among 32–52 atoms. This dilution of the excess charges decreases the magnitude of the Coulomb force and partially compensates for the increase due to the lack of dielectric medium between the contact ion-pairs.

Additionally, Eq. 2 only models the Coulomb interaction and does not account for changes in solvation energy upon ion pairing, as pointed out by Tachiya.[21] To address this, we attempted to estimate the contribution of desolvation to C_{MD} in ACN by simulating the PMFs for $\mathrm{A}^{\cdot-}/\mathrm{D}$ and $\mathrm{A}/\mathrm{D}^{\cdot+}$ in ACN and HEX, functions we term $w_{\mathrm{mix}}(r)$. These simulations are described in detail in Section S6. In HEX, where no dipolar solvation can occur, $w_{\mathrm{mix}}(r)$ accounts for the self-interaction between the constituents of the charged/neutral pair. By subtracting $w_{\mathrm{mix}}(r)$ in HEX from that calculated in ACN we can estimate the pure ACN contribution to the free energy. This difference, $\Delta w_{\mathrm{mix}}(r)$, reflects how the solvation energy of an ion is affected upon approaching a molecule of the same size as the counterion but without a charge. By summing the values of $\Delta w_{\mathrm{mix}}(r)$ for $\mathrm{A}^{\cdot-}/\mathrm{D}$ and $\mathrm{A}/\mathrm{D}^{\cdot+}$ at $r = r_{\mathrm{MD}}$ we

can estimate the solvation energy of the pair at contact. Such $\Delta w_{\mathrm{mix}}(r)$ for SPH/SPH and DMA/PER are shown in Figure 3 and the constituent $w_{\mathrm{mix}}(r)$ in Figures S8 and S9. According to these calculations, the loss of solvation energy in ACN upon bringing $\mathrm{SPH}^{+}/\mathrm{SPH}^{-}$ into contact is on the order of 0.13 eV. Although this desolvation energy is not negligible when compared to C_{MD}, it is very small when compared to the solvation energy of the two spherical ions in ACN of 8 eV, as calculated from the Born equation. This reflects the fact that dipolar solvation is a long-range interaction that goes far beyond the first solvent shell. Consequently, even though the ions are in contact, a non-negligible screening of the charges by the solvent can occur.

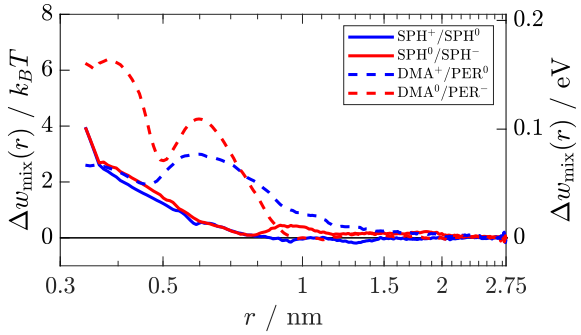

Figure 3: Differences between the potentials of mean force in ACN and HEX for $\mathrm{A}^{\cdot-}/\mathrm{D}$ and $\mathrm{A}/\mathrm{D}^{\cdot+}$ $\Delta w_{\mathrm{mix}}(r)$, for the SPH/SPH and PER/DMA pairs. These $\Delta w_{\mathrm{mix}}(r)$ reflect the loss of solvation energy of the ion upon approaching a molecule of the same size as the counterion but without a charge.

For the DMA/PER pair, the decrease of solvation energy upon bringing $\mathrm{DMA}^{\cdot+}$ and $\mathrm{PER}^{\cdot-}$ to the most stable sandwich geometry amounts to about 9 $k_{\mathrm{B}}T$ (0.23 eV). Given that $C_{\mathrm{MD}} = -0.17\,\mathrm{eV}$, the purely Coulombic stabilization of $\mathrm{PER}^{\cdot-}$ and $\mathrm{DMA}^{\cdot+}$ pair is on the order of -0.4 eV in ACN and about -0.53 eV, for $\mathrm{SPH}^{+}/\mathrm{SPH}^{-}$, values significantly larger than those calculated from Eq. 2. Consequently, these results suggest that the ability of Eq. 2 to provide good estimates of C when using the proper contact distance is fortuitous and is due to the interplay of three main factors: i) the underestimation of the Coulomb energy at contact due to overestimation of the dielectric screening, ii) dilution of charge among the constituent atoms of the molecular ions, and iii) neglecting the decrease of solvation energy upon ion pairing.

4 Conclusions

Our simulations have revealed that the contribution of the self-interaction term C in the ET driving force is underestimated by a factor 2 when calculated using the traditional Weller equation method. Practically, this means that in a highly polar solvent, such as ACN, ΔG_{ET} is 0.10-15 eV more negative than normally calculated and cannot be neglected. This underestimation can be compensated for by using the π-stack contact distance of 0.37 nm, which provides a significantly better prediction for C than the van der Waals radius of the pair. In medium polarity solvents such as DCM, it is even more important to use r_{MD} to calculate C, as the absolute differences between C_{MD} and $C(r_{\mathrm{vdW}})$ are a factor of 4 greater than in ACN. Selecting an improper value of C can change the predicted values of k_{ET} by several orders of magnitude. The agreement between C_{MD} and $C(r_{\mathrm{MD}})$ is most likely fortuitous due the compensating effects of overestimating the dielectric screening and of neglecting both desolvation and excess charge dilution in molecular ions. Our simulations also suggest that the concept of solvent-separated ion-pairs as well-defined transient species can be applied to atomic ions, but not to the molecular ions usually produced upon bimolecular photoinduced ET. Further studies of D/A pair structures using MD simulations and their effect on the electronic coupling and reaction free energy surfaces will be described a forthcoming paper.

Acknowledgement

The authors thank the Fonds National Suisse de la Recherche Scientifique (Project Nr. 200020-184607) as well as the University of Geneva for financial support. All molecular dynamics simulations were performed on the Baobab cluster at the University of Geneva.

Supporting Information Available

Supplementary Information: computational details and additional data. The data can be downloaded from http://doi.org/10.5281/zenodo.3999116. This material is available free of charge via the Internet at `http://pubs.acs.org/`.

References

(1) Bixon, M.; Jortner, J. Electron Transfer - from Isolated Molecules to Biomolecules. *Adv. Chem. Phys.* **1999**, *106*, 35–202.

(2) Mataga, N.; Miyasaka, H. Electron Transfer and Exciplex Chemistry. *Adv. Chem. Phys.* **1999**, *107*, 431–496.

(3) Balzani, V. *Electron Transfer in Chemistry*; J. Wiley: New York, 2001.

(4) Wasielewski, M. R. M. Self-Assembly Strategies for Integrating Light Harvesting and Charge Separation in Artificial Photosynthetic Systems. *Acc. Chem. Res.* **2009**, *42*, 1910–21.

(5) Clarke, T. M.; Durrant, J. R. Charge Photogeneration in Organic Solar Cells. *Chem. Rev.* **2010**, *110*, 6736–6767.

(6) Bottari, G.; de la Torre, G.; Guldi, D. M.; Torres, T. Covalent and Noncovalent Phthalocyanine-Carbon Nanostructure Systems: Synthesis, Photoinduced Electron Transfer, and Application to Molecular Photovoltaics. *Chem. Rev.* **2010**, *110*, 6768–6816.

(7) Prier, C. K.; Rankic, D. A.; MacMillan, D. W. C. Visible Light Photoredox Catalysis with Transition Metal Complexes: Applications in Organic Synthesis. *Chem. Rev.* **2013**, *113*, 5322–5363.

(8) Heeger, A. J. 25th Anniversary Article: Bulk Heterojunction Solar Cells: Understanding the Mechanism of Operation. *Adv. Mater.* **2014**, *26*, 10–28.

(9) Ashford, D. L.; Gish, M. K.; Vannucci, A. K.; Brennaman, M. K.; Templeton, J. L.; Papanikolas, J. M.; Meyer, T. J. Molecular Chromophore-Catalyst Assemblies for Solar Fuel Applications. *Chem. Rev.* **2015**, *115*, 13006–13049.

(10) Hammarström, L. Accumulative Charge Separation for Solar Fuels Production: Coupling Light-Induced Single Electron Transfer to Multielectron Catalysis. *Acc. Chem. Res.* **2015**, *48*, 840–850.

(11) Kumpulainen, T.; Lang, B.; Rosspeintner, A.; Vauthey, E. Ultrafast Elementary Photochemical Processes of Organic Molecules in Liquid Solution. *Chem. Rev.* **2017**, *117*, 10826–10939.

(12) Koyama, D.; Dale, H. J. A.; Orr-Ewing, A. J. Ultrafast Observation of a Photoredox Reaction Mechanism: Photoinitiation in Organocatalyzed Atom-Transfer Radical Polymerization. *J. Am. Chem. Soc.* **2018**, *140*, 1285–1293.

(13) Corrigan, N.; Xu, J.; Boyer, C.; Allonas, X. Exploration of the PET-RAFT Initiation Mechanism for Two Commonly Used Photocatalysts. *ChemPhotoChem* **2019**, *3*, 1193–1199.

(14) Marcus, R. A.; Sutin, N. Electron Transfer in Chemistry and Biology. *Biochim. Biophys. Acta* **1985**, *811*, 265–322.

(15) Rehm, D.; Weller, A. Kinetic of Fluorescence Quenching by Electron and Hydrogen Atom Transfer. *Isr. J. Chem.* **1970**, *8*, 259–271.

(16) Weller, A. Photoinduced Electron Transfer in Solutions: Exciplex and Radical Ion Pair Formation Free Enthalpies and their Solvent Dependence. *Z. Phys. Chem.* **1982**, *133*, 93–98.

(17) Jones, W. E.; Fox, M. A. Determination of Excited-State Redox Potentials by Phase-Modulated Voltammetry. *J. Phys. Chem.* **1994**, *98*, 5095–5099.

(18) Gould, I. R.; Ege, D.; Mattes, S.; Farid, S. Return Electron Transfer within Geminate Radical Ion Pair. Observation of the Marcus Inverted Region. *J. Am. Chem. Soc.* **1987**, *109*, 3794–3796.

(19) Kikuchi, K.; Takahashi, Y.; Hoshi, M.; Niwa, T.; Katagiri, T.; Miyashi, T. Free Enthalpy Dependence of Free Radical Yield of Photoinduced Electron Transfer in Acetonitrile. *J. Phys. Chem.* **1991**, *95*, 2378.

(20) Suppan, P. The Importance of the Electrostatic Interaction in Condensed-Phase Photoinduced Electron Transfer. *J. Chem. Soc. Far. Trans. 1* **1986**, *82*, 509–511.

(21) Tachiya, M. Energetics of Electron Transfer Reactions in Polar Solvents. *Chem. Phys. Lett.* **1994**, *230*, 491–494.

(22) Willemse, R. J.; Verhoeven, J. W.; Brouwer, A. M. Reversible Charge Migration in the Excited State of an Electron Donor-Donor-Acceptor System Detected via Delayed Charge Transfer Fluorescence. *J. Phys. Chem.* **1995**, *99*, 5753–5756.

(23) Koch, M.; Letrun, R.; Vauthey, E. Exciplex Formation in Bimolecular Photoinduced Electron-Transfer Investigated by Ultrafast Time-Resolved Infrared Spectroscopy. *J. Am. Chem. Soc.* **2014**, *136*, 4066–4074.

(24) Kikuchi, K.; Niwa, T.; Takahashi, Y.; Ikeda, H.; Miyashi, T.; Hoshi, M. Evidence of Exciplex Formation in Acetonitrile. *Chem. Phys. Lett.* **1990**, *173*, 421–424.

(25) Gould, I. R.; Young, R. H.; Mueller, L. J.; Farid, S. Mechanism of Exciplex formation. Role of Superexchange, Solvent Polarity, and Driving Force for Electron Transfer. *J. Am. Chem. Soc.* **1994**, *116*, 8176–8187.

(26) Kuzmin, M. G. M.; Soboleva, I. V. I.; Dolotova, E. V. E.; Dogadkin, D. N. D. Evidence for Diffusion-Controlled Electron Transfer in Exciplex Formation Reactions. Medium Reorganisation Stimulated by Strong Electronic Coupling. *Photochem. Photobiol. Sci.* **2003**, *2*, 967–974.

(27) Dossot, M.; Allonas, X.; Jacques, P. Singlet Exciplexes between a Thioxanthone Derivative and Substituted Aromatic Quenchers: Role of the Resonance Integral. *Chem. Eur. J.* **2005**, *11*, 1763–1770.

(28) Murata, S.; Tachiya, M. Unified Interpretation of Exciplex Formation and Marcus Electron Transfer on the Basis of Two-Dimensional Free Energy Surfaces. *J. Phys. Chem. A* **2007**, *111*, 9240–9248.

(29) Nançoz, C.; Rumble, C.; Rosspeintner, A.; Vauthey, E. Bimolecular Photoinduced Electron Transfer in Non-Polar Solvents beyond the Diffusion Limit. *J. Chem. Phys.* **2020**, *152*, 244501.

(30) Angel, S. A.; Peters, K. S. Free Energy Dependence of the Intrinsic Rate of Electron Transfer in Diffusional Quenching of Trans-Stilbene S1 by Electron-Deficient Olefins. *J. Phys. Chem.* **1991**, *95*, 3606–3612.

(31) Vauthey, E.; Henseler, A. Picosecond Transient Thermal Phase Grating Study of a Photoinduced Electron Transfer Reaction in Solution. *J. Phys. Chem.* **1995**, *99*, 8652–8660.

(32) Vauthey, E.; Henseler, A. Application of Transient Grating Spectroscopy to the Study of the Energetics and Dynamics of Electron Transfer Reaction: Separation of an Ion Pair into Free Ions. *J. Photochem. Photobiol. A* **1998**, *112*, 103–109.

(33) Carter, E. A.; Hynes, J. T. Solute-Dependent Solvent Force Constants for Ion Pairs and Neutral Pairs in a Polar Solvent. *J. Phys. Chem.* **1989**, *93*, 2184–2187.

(34) King, G.; Warshel, A. Investigation of the Free Energy Functions for Electron Transfer Reactions. *J. Chem. Phys.* **1990**, *93*, 8682–8692.

(35) Ando, K. Photoinduced Intermolecular Electron Transfer Reaction between N,N-Dimethylaniline and Anthracene in Acetonitrile Solution: A Theoretical Study. *J. Chem. Phys.* **1994**, *101*, 2850–2862.

(36) Hilczer, M.; Tachiya, M. Effect of Solvent Polarity on the Potential of Mean Force between two Molecular Ions: MD Simulation. *Chem. Phys. Lett.* **1998**, *295*, 337–346.

(37) Jorgensen, W. L.; Maxwell, D. S.; Tirado-Rives, J. Development and Testing of the OPLS All-Atom Force Field on Conformational Energetics and Properties of Organic Liquids. *J. Am. Chem. Soc.* **1996**, *118*, 11225–11236.

(38) Price, M. L. P.; Ostrovsky, D.; Jorgensen, W. L. Gas-Phase and Liquid-State Properties of Esters, Nitriles, and Nitro Compounds with the OPLS-AA Force Field. *J. Comput. Chem.* **2001**, *22*, 1340–1352.

(39) Rumble, C. A.; Vauthey, E. Structural Dynamics of an Excited DonorAcceptor Complex from Ultrafast Polarized Infrared Spectroscopy, Molecular Dynamics Simulations, and Quantum Chemical Calculations. *21*, 11797–11809.

(40) Masnovi, J. M.; Kochi, J. K. Direct Observation of Ion Pair Dynamics. *J. Am. Chem. Soc.* **1985**, *107*, 7880–7893.

(41) Gould, I.; Young, R.; Moody, R.; Farid, S. Contact and Solvent-Separated Geminate Radical Ion Pairs in Electron Transfer Photochemistry. *J. Phys. Chem.* **1991**, *95*, 2068–2080.

(42) Peters, K. S.; Lee, J. Role of Contact and Solvent Separated Radical Ion Pairs in the Diffusional Quenching of Trans-Stilbene Excited State by Fumaronitrile. *J. Phys. Chem.* **1992**, *96*, 8941–8945.

(43) Burshtein, A. Unified Theory of Photochemical Charge Separation. *Adv. Chem. Phys.* **2000**, *114*, 419–587.

(44) Saik, V. O.; Goun, A. A.; Nanda, J.; Shirota, K.; Tavernier, H. L.; Fayer, M. D. Photoinduced Intermolecular Electron Transfer in Liquid Solutions. *J. Phys. Chem. A* **2004**, *108*, 6696–6703.

(45) Angulo, G.; Rosspeintner, A.; Lang, B.; Vauthey, E. Optical Transient Absorption Experiments Reveal the Failure of Formal Kinetics in Diffusion Assisted Electron Transfer Reactions. *Phys. Chem. Chem. Phys.* **2018**, *20*, 25531 – 25546.

Graphical TOC Entry